L-Arginine currents in rat cardiac ventricular myocytes

R. Daniel Peluffo

Department of Pharmacology and Physiology, University of Medicine and Dentistry of New Jersey, New Jersey Medical School, Newark, NJ 07101, USA

L-Arginine (L-Arg) is a basic amino acid that plays a central role in the biosynthesis of nitric oxide, creatine, agmantine, polyamines, proline and glutamate. Most tissues, including myocardium, must import L-Arg from the circulation to ensure adequate intracellular levels of this amino acid. This study reports novel L-Arg-activated inward currents in whole-cell voltage-clamped rat ventricular cardiomyocytes. Ion-substitution experiments identified extracellular L-Arg as the charge-carrying cationic species responsible for these currents, which, thus, represent L-Arg import into cardiac myocytes. This result was independently confirmed by an increase in myocyte nitric oxide production upon extracellular application of L-Arg. The inward movement of Arg molecules was found to be passive and independent of Na^+, K^+, Ca^{2+} and Mg^{2+}. The process displayed saturation and membrane potential (V_m)-dependent kinetics, with a $K_{0.5}$ for L-Arg that increased from 5 mM at hyperpolarizing V_m to 20 mM at +40 mV. L-Lysine and L-ornithine but not D-Arg produced currents with characteristics similar to that activated by L-Arg indicating that the transport process is stereospecific for cationic L-amino acids. L-Arg current was fully blocked after brief incubation with 0.2 mM *N*-ethylmaleimide. These features suggest that the activity of the low-affinity, high-capacity CAT-2A member of the y^+ family of transporters is responsible for L-Arg currents in acutely isolated cardiomyocytes. Regardless of the mechanism, we hypothesize that a low-affinity arginine transport process in heart, by ensuring substrate availability for sustained NO production, might play a cardio-protective role during catabolic states known to increase Arg plasma levels severalfold.

(Received 16 November 2006; accepted after revision 13 February 2007; first published online 15 February 2007)
Corresponding author R. D. Peluffo: Department of Pharmacology and Physiology, University of Medicine and Dentistry of New Jersey, 185 South Orange Avenue, PO Box 1709, Newark, NJ 07101-1709, USA. Email: peluffrd@umdnj.edu

Arginine (Arg) is a cationic amino acid which is essential for optimal physiological growth and also during catabolic states such as trauma, severe burns, stress, sepsis and starvation. In addition to its role as a building block for protein synthesis, Arg stimulates the release of hormones such as insulin, glucagon, growth hormone and prolactin (reviewed in Devés & Boyd, 1998), and is a precursor in the synthesis of urea, creatine, agmatine and polyamines such as spermine and putrescine, known to be involved in inward rectification of K^+ channels in nerve and muscle (reviewed in Aidley & Stanfield, 1996). The role of nitric oxide (NO) as a major regulator in the nervous, immune and cardiovascular systems (Bredt & Snyder, 1994) also highlights the importance of its sole precursor, L-Arg, via nitric oxide synthase (NOS). In the heart, NO generated by cardiac myocytes decreases the rate of spontaneous beating and the velocity and extent of shortening (Balligand *et al.* 1993), and accelerates the velocity of re-lengthening (Grocott-Mason *et al.* 1994). NO also plays roles in hypertrophy and apoptosis of cardiomyocytes. Interestingly, alterations of the Arg–NO pathway have been reported in chronic heart failure (Mendes Ribeiro *et al.* 2001).

The effects described above for Arg and NO require the presence of this amino acid in the intracellular milieu of responsive tissues. While some cell types can synthesize Arg from ornithine or citrulline (Hecker *et al.* 1990; Wu & Brosnan, 1992), most tissues, including cardiac muscle, lack the biochemical machinery for the *de novo* synthesis of this amino acid or its recycling from citrulline pools (Hattori *et al.* 1995; Nagasaki *et al.* 1996). As a consequence, Arg must be transported into these tissues from the circulation to ensure adequate intracellular levels of this multifunctional amino acid. An example of this is the increased capacity for Arg transport that occurs in parallel with the expression of inducible NOS in various cell types in order to support NO synthesis (Simmons *et al.* 1996). Clearly, the molecular mechanism responsible for Arg import must be of central importance in the metabolism of this amino acid and NO.

Five transport systems for cationic amino acids, termed b^+, $b^{0,+}$, $B^{0,+}$, y^+L and y^+, have been described in different cell types and tissues. All five systems move charge across the cell membrane electric field generating electrical currents as a result of their cationic amino acid transport

 DOI: 10.1113/jphysiol.2006.125054

activity. System b^+, first described in preimplantation mouse blastocysts, is specific for cationic amino acids (Van Winkle & Campione, 1990). Systems $b^{0,+}$ and $B^{0,+}$, on the other hand, transport dibasic as well as neutral amino acids, the former in a Na^+-independent fashion, the latter in a strictly Na^+-dependent manner (reviewed in Devés & Boyd, 1998). System y^+L transports cationic amino acids in the absence of Na^+ and, unlike system $b^{0,+}$, it transports neutral amino acids in a Na^+-dependent manner. It must be pointed out that systems b^+, $b^{0,+}$, $B^{0,+}$ and y^+L all mediate high-affinity cationic amino acid transport with $K_{0.5}$-values ranging from 3 to 150 μM (Devés & Boyd, 1998).

Finally, the system y^+ family of transporters (CAT) is highly selective for cationic L-amino acids and its transport activity is Na^+ independent (Christensen, 1964). Moreover, amino acid transport mediated by members of this system is also independent of external K^+, Ca^{2+}, or Mg^{2+} (Kim *et al.* 1991; Kakuda *et al.* 1993; Nawrath *et al.* 2000). System y^+ includes the high-affinity CAT-1, CAT-2B and CAT-3 ($K_{0.5}$ for Arg, 100–250 μM) as well as the low-affinity CAT-2A ($K_{0.5}$ for Arg, 2–5 mM) (see Devés & Boyd, 1998; and references therein). An additional member, CAT-4, described in human brain, placenta and testis, has not been characterized in terms of an apparent affinity for Arg activation (Sperandeo *et al.* 1998). In rat, CAT-1 is expressed ubiquitously except in the liver where CAT-2A is the only isoform present (MacLeod & Kakuda, 1996). In neonatal rat hearts, it has been reported that cardiac myocytes constitutively exhibit CAT-1 transport activity and that a 24 h-long treatment with cytokines induces also CAT-2A and CAT-2B expression and a correspondingly enhanced Arg uptake (Simmons *et al.* 1996).

Arg transport has been previously measured in mouse pancreatic β-cells using voltage-clamp techniques (Smith *et al.* 1997). However, the magnitude of the current generated by this process was, at best, 0.5 pA pF^{-1} (10 mM L-Arg, −70 mV). We report up to eightfold larger current densities produced by millimolar concentrations of extracellular L-Arg in freshly isolated cardiac ventricular myocytes from adult rats. The size of these currents encouraged initial biochemical and biophysical characterization of cardiac Arg transport in its native environment.

Parts of this work have been previously published in abstract form (Peluffo, 2004, 2005).

Methods

Adult male rats were injected with Nembutal, 100 mg kg^{-1} I.P., in accordance with the guidelines of the Institutional Animal Care and Use Committee of the New Jersey Medical School. Hearts were removed under complete anaesthesia and single ventricular myocytes were enzymatically isolated following published methods (Mitra & Morad, 1985).

Whole-cell voltage-clamp experiments

Cells were placed in a superfusion chamber on the stage of an inverted microscope and superfused at 36 ± 1°C with a Tyrode solution containing (mM): 145 NaCl, 5 KCl, 10 dextrose, 2 $CaCl_2$, 1 $MgCl_2$, 10 Hepes–NaOH, pH 7.40 (23°C). Myocytes were then whole-cell voltage-clamped with low-resistance (1.0–1.5 MΩ) patch electrodes back-filled with an intracellular salt solution containing (mM): 110 potassium aspartate, 20 TEACl, 4 $MgCl_2$, 0.7 MgATP, 10 EGTA–Tris, 5 glucose, 10 Hepes–KOH, pH 7.30 (23°C).

After establishing a gigaohm seal, the superfusion solution was switched to a Na^+- and K^+-free solution containing (mM): 145 tetramethylammonium chloride (TMACl), 2.3 $MgCl_2$, 0.2 $CdCl_2$, 5.5 dextrose, 10 Hepes–Tris, pH 7.40 (23°C). L-Arginine (L-Arg)-containing solutions were prepared by equimolar substitution of TMA. Extracellular TMA and Cd^{2+} as well as intracellular TEA were added to block contaminating ionic currents. Voltage-clamped myocytes were exposed to these blocking agents for 5 min before further manipulations.

Voltage-clamp protocol

To study the V_m dependence of L-Arg-activated currents, step changes in V_m with a duration of 100 ms were produced from a holding potential of −40 mV to various potentials over the range of −100 to +40 mV at 2 Hz. These voltage jumps were applied before and during superfusion with L-Arg-containing solution, and again after withdrawal of L-Arg, to obtain the respective current–V_m relationships. Current–V_m curves obtained before application and after removal of L-Arg showed small differences in slope and were usually averaged. L-Arg-activated currents were defined as the difference between current levels measured in the absence and presence of the various L-Arg concentrations described in the text.

Giant excised-patch technique

Inside-out patches were obtained as described by Hilgemann (Hilgemann, 1989; Collins *et al.* 1992) with minor modifications. In brief, cardiac myocytes were incubated during ∼10 min with a hypotonic 'storage' solution (mM: 67 KCl, 5 EGTA, 5 glucose, 1 $MgCl_2$, 5 Hepes–KOH, pH 7.40 at 23°C) to promote acute membrane bleb formation. Once blebs were formed, cells

were dispersed in an experimental chamber containing a 'seal' solution (mM: 100 potassium aspartate, 20 KCl, 2 EGTA, 4 $MgCl_2$, 10 Hepes–KOH, pH 7.00 at 23°C). Blebs approximately 25% the size of the cell were approached with single patch electrodes (tip diameter, 7–15 μm) back-filled with an electrode salt solution (see superfusion solution for whole-cell voltage-clamp experiments above). Electrodes were coated with α-tocopherol to decrease stray capacitance and improve seal characteristics.

After forming a gigaohm seal, membrane patches were excised and positioned in a superfusion chamber at 37°C. Intracellular L-Arg-activated currents were recorded by superfusing the patches with a bath solution of composition identical to that described as intracellular salt solution for whole-cell voltage-clamp experiments. Potassium aspartate was substituted for L-Arg in equimolar amounts, as needed.

Fluorescence measurements

To detect nitric oxide release, freshly isolated cardiac myocytes suspended in Tyrode solution were loaded (60 min at 37°C) with 10 μM of the dye DAF-FM diacetate (4 - amino - 5 - methylamino - 2′,7′-difluorofluorescein diacetate; λ_{ex} = 495 nm, λ_{em} = 515 nm). The fluorescence quantum yield of DAF-FM increases greatly after reacting with NO to form a benzotriazole derivative. The status of the cells after many manipulations (incubations, resuspensions, centrifugations) and DAF-FM loading as well as the dye distribution and reactivity were monitored by confocal microscopy (PCM 2000, Nikon Inc.).

Data analysis

Current traces shown in Figs 1, 3, 5 and 6, recorded at the holding potential, were sampled at 25 Hz and low-pass filtered at 5 Hz. Current traces shown in Fig. 1*B* were sampled at 5 kHz and low-pass filtered at 1 kHz. Linear cell capacitance, 124 ± 5 pF (n = 27), was calculated with Clampex (Molecular Devices Corp., Sunnyvale, CA, USA) using 5 mV depolarizations. Unless otherwise stated, data are displayed as mean ± S.E.M. for the indicated number of experiments. Statistical significance ($P < 0.05$) was evaluated using Student's t tests. Curve fitting was carried out by non-linear least-squares routines using Clampfit (Molecular Devices Corp., Sunnyvale, CA, USA) or SigmaPlot v8.0 (SPSS, Chicago, IL, USA).

Equipment and reagents

Voltage-clamp experiments were performed with a low-noise Axopatch 200B patch-clamp amplifier using a Digidata 1320 and pCLAMP 8.0.2 software for data acquisition and analysis (all from Molecular Devices Corp.). Fluorescence measurements were carried out with a Cary Eclipse Spectrofluorometer. DAF-FM diacetate was from Molecular Probes. Hydrochloride salts of L-arginine, D-arginine, L-lysine, and L-ornithine, as well as all other chemicals, were from Sigma-Aldrich.

Results

Extracellular L-arginine (L-Arg_o)-activated current in cardiac myocytes

An inwardly directed current was observed in freshly isolated rat cardiac ventricular myocytes that were whole-cell voltage clamped with patch electrodes containing a high K^+ intracellular salt solution and superfused with a Na^+- and K^+-free, 10 mM L-Arg_o-containing solution (Fig. 1*A*). The magnitude of this current was typically in the range 120–160 pA at the holding membrane potential (V_m) of −40 mV. To study the V_m dependence of these currents, the voltage-clamp protocol described in Methods was applied before adding L-Arg and again in the presence of the amino acid. Upon subtraction, the family of L-Arg_o-sensitive current traces shown in Fig. 1*B* was obtained. Average current values calculated for the last 70 ms of the applied voltage pulses were defined as steady-state current levels and plotted as a function of V_m to generate the corresponding current (I_m)–V_m relationship (Fig. 1*C*). Inward current amplitude densities reached minimal values at positive V_m and increased exponentially, in absolute value, at more negative potentials showing no signs of saturation at up to −100 mV. Data in Fig. 1*C* were fitted with the following empirical function,

$$I_m = I_0 \exp(-\lambda z F V_m / RT) + I_\infty \quad (1)$$

where I_0 represents $(I_m - I_\infty)$ at V_m = 0; λ accounts for the steepness of the I_m–V_m curve; I_∞ is the value of I_m at V_m approaching $+\infty$; z is valency; F, Faraday constant; R, the universal gas constant; and T is absolute temperature. Assuming $z = 1$, best-fit values for I_0, λ and I_∞ were found to be -0.37 ± 0.03 pA pF^{-1}, 0.56 ± 0.02 and -0.17 ± 0.03 pA pF^{-1}, respectively. The V_m-dependent behaviour of current observed in Fig. 1 is consistent with either the inward movement of positive charges or the outward movement of negative charges.

The identity of the charge-carrying species

A key question is whether Arg is the charge-carrying species in these L-Arg-activated currents. Experimental solutions contained ion channel blockers, so that Arg-sensitive currents could be studied in the absence of contaminating ionic currents (see Methods). Typically, tetramethylammonium ion (TMA) and L-Arg were the

only ionic species with a net charge of +1 in the superfusion solution. A putative L-Arg-activated TMA inward transport/permeation process was ruled out in three ion-substitution experiments where replacement of 140 mM TMACl with equimolar NaCl or KCl had little (< 10%) effect on current density levels (not shown).

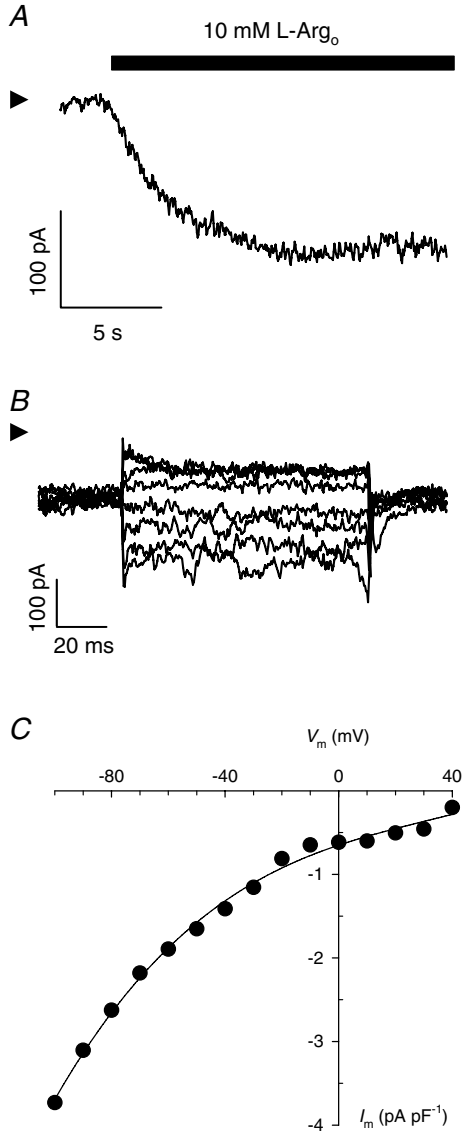

Figure 1. Extracellular L-Arg-activated currents in cardiac myocytes
A, inward current produced by application of 10 mM L-Arg$_o$ at the holding potential of −40 mV. Current was measured at 36°C in a myocyte whole-cell voltage clamped with a low-resistance patch electrode containing a high-K^+ intracellular salt solution. *B*, L-Arg-sensitive difference currents. Superimposed current traces are shown for V_m jumps to −80, −70, −60, −50, −30, −20, 0 and +20 mV. *C*, I_m–V_m relationship. Data points represent average current density levels calculated for the last 70 ms of each trace. Equation (1) was fitted to the data. Arrowheads in *A* and *B* indicate zero-current levels. Cell capacitance: 114 pF. Summarized results for five cells are presented in Fig. 5.

As for Cd^{2+} (200 μM) and Mg^{2+} (2 mM), also present in the extracellular solution, the former is a potent, non-permeating channel blocker, and replacement of the latter with 2 mM Ca^{2+} did not affect L-Arg-activated current (not shown). These findings also imply that Na^+, K^+ and Ca^{2+} channels were not involved in the occurrence of L-Arg-activated currents.

The relevant anionic species that could produce outward movement of negative charges are chloride and aspartate (K^+ counterion in the electrode solution). In the case of Cl^-, the ratio of extra- and intracellular chloride concentrations used in the experiments yields a reversal potential of −45 mV at 37°C, very close to our working holding potential (−40 mV). Thus, outward movement of Cl^- could not account for the current amplitude shown in Fig. 1*A*. With regard to aspartate (Asp), its concentration gradient ($[Asp]_{pip}$ = 110 mM; $[Asp]_o$ = 0 mM) will favour the outward movement of negative charges. Thus, experiments measuring L-Arg$_o$-activated current in the presence of 50 mM Asp$_o$ were performed to test whether L-Arg$_o$ triggered outward displacement of intracellular Asp. Under these conditions, smaller current amplitudes are anticipated because of the smaller Asp electrochemical potential gradient. No effect of Asp$_o$ on current levels was found in two such experiments (not shown).

Together, these observations strongly suggest that L-Arg-activated currents are generated by the inward movement of L-Arg molecules into cardiac myocytes. Nonetheless, additional independent evidence supporting L-Arg import in this cell type is presented below.

Nitric oxide production induced by millimolar concentrations of extracellular L-Arg

Since L-Arg is the sole substrate for nitric oxide synthase (NOS) activity, production of NO will demonstrate the influx of L-Arg molecules. To detect NO release, fluorescence spectroscopic studies were conducted in cardiomyocytes loaded with the dye DAF-FM (Kojima *et al.* 1998*a*,*b*). The non-fluorescent DAF-FM diacetate passively diffuses across the cell membrane and is deacetylated by intracellular esterases to become the weakly fluorescent DAF-FM (Fig. 2*A*, left). The fluorescence quantum yield of DAF-FM increases greatly after reacting with NO, a point confirmed by confocal fluorescence imaging of DAF-FM-loaded myocytes exposed to the NO donor, sodium nitroprusside (Fig. 2*A*, right). These studies also serve as a control for the healthy status of the cells after several experimental manipulations and DAF-FM loading.

To follow L-Arg uptake, the effect of L-Arg on fluorescence intensity changes was measured. Results in Fig. 2*B* show a clear, sustained increase in fluorescence

intensity (i.e. NO production) upon addition of 15 mM L-Arg_o to myocytes that were preincubated for at least 1 h with 10 μM DAF-FM diacetate (filled circles). This effect was not observed in parallel assays where L-Arg was replaced with either 15 mM D-Arg (open circles) or vehicle (filled triangles). NOS specificity for the L-isomer of arginine is well documented (Hobbs *et al.* 1999). However, the possibility that arginine import is also a stereospecific process cannot be ruled out by these experiments (but see Fig. 4). Preincubation of myocytes with 1 mM L-NAME, a NOS inhibitor, completely abolished the effect of 15 mM L-Arg on fluorescence intensity (open triangles), a finding that confirms the involvement of NOS activity in the fluorescence increase upon L-Arg addition. These results strongly suggest that L-Arg was transported into cardiac myocytes and converted by endogenous NOS into its product, NO.

The driving force behind L-Arg_o-activated current

Having established L-Arg import as the charge-carrying event behind L-Arg-activated currents, the next question was whether L-Arg is crossing the myocyte plasma membrane actively or passively. In this regard, although ATP was usually included in the electrode solution to avoid opening of K_{ATP} channels, three control experiments performed in the presence of 10 μM glyburide (Nichols & Lederer, 1991) with no added glucose and ATP suggested that a primary source of energy is not required for the occurrence of L-Arg-activated currents (not shown). Thus, the movement of L-Arg molecules across the cardiac myocyte plasma membrane does not seem to represent a primary active process and, since the presence of Na^+ or Ca^{2+} gradients is not needed for L-Arg-activated currents (see above), a secondary active process also does not appear to be likely.

The chief feature of passive transport processes is that substances move along their electrochemical potential gradients. If this is the case, a 'zero-*trans*' experiment, similar to that described in Fig. 1 but adding intracellular rather than extracellular L-Arg, is anticipated to elicit outward current. This prediction was tested with giant inside-out patches excised from cardiac myocytes, a technique that permits biochemical control at both sides of the plasma membrane. Briefly, membrane blebs were formed by exposing myocytes to a hypotonic salt solution (see Methods) and a membrane patch was excised from the selected cell and voltage-clamped at a holding potential of +40 mV. Upon superfusion with an intracellular solution containing 10 mM L-Arg (L-Arg_i), an outwardly directed current (whole-cell convention) approximately 20 pA in size, was apparent (Fig. 3*A*). This current amplitude is comparable in magnitude to those reported for the functioning of the cardiac Na^+–K^+ pump and Na^+–Ca^{2+} exchanger in giant excised patches (Collins *et al.* 1992). Application of the voltage-jump protocol in the absence and presence of L-Arg_i resulted, after subtraction, in the I_m–V_m relationship shown in Fig. 3*B*. Fitting this I_m–V_m curve with eqn (1) yielded a value of $\lambda = 0.53 \pm 0.04$, not significantly different from that reported above for the steepness of the inward I_m–V_m relationship obtained with intact voltage-clamped myocytes. Figure 3*B* also shows that outward current densities are similar in absolute value to inward current levels measured with the whole-cell voltage-clamp technique (Fig. 1*C*).

Two additional membrane patches of comparable sizes yielded current levels of 17 and 22 pA at +40 mV

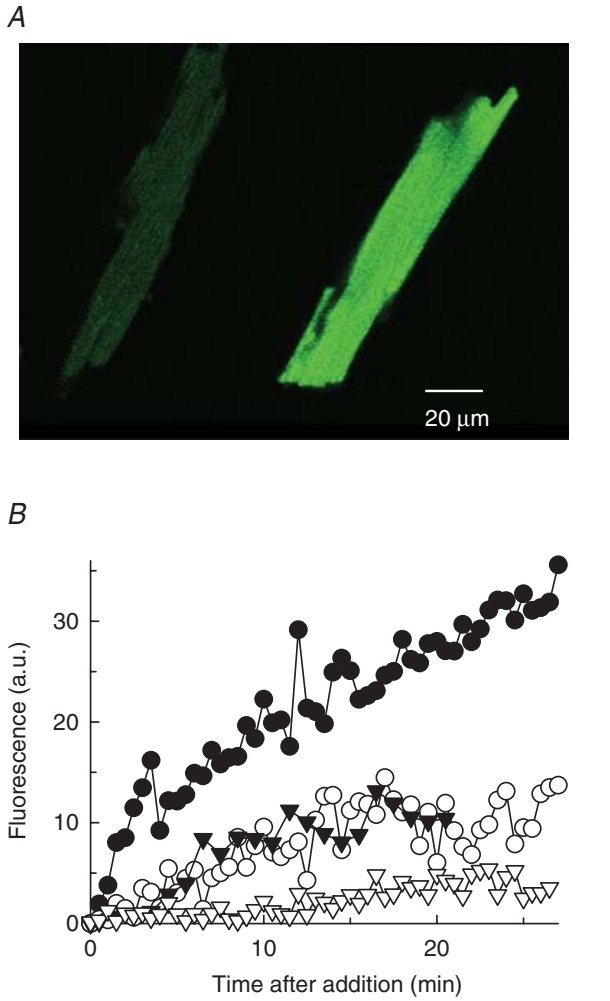

Figure 2. Measurement of NO production in cardiac myocytes
A, confocal fluorescence images. DAF-FM-loaded cardiac myocytes showed an increase in fluorescence (average pixel value) from 31 ± 4 (n = 6) in the absence (left) to 168 ± 16 (n = 7) in the presence of the NO donor, sodium nitroprusside (right). *B*, specificity of NO production on L-Arg. Time courses of fluorescence intensity changes (in arbitrary units) in DAF-FM-loaded myocytes upon addition of 15 mM L-Arg (●), 15 mM D-Arg (○), an equal volume of Arg-free buffer (▼), or 15 mM L-Arg in cells preincubated with 1 mM L-NAME (▽). The low-level, basal NO production (filled *versus* open triangles) is probably due to L-Arg intracellular pools.

and λ-values for the I_m–V_m curves of 0.55 ± 0.02 and 0.50 ± 0.04, respectively. Thus, outward movement of Arg molecules takes place with a capacity and V_m dependence similar to those for Arg import. The main conclusion to be drawn from these experiments is that Arg molecules move passively, i.e. along their electrochemical potential gradient in cardiac myocytes.

Selectivity of inwardly directed currents for the L-isomers of cationic amino acids

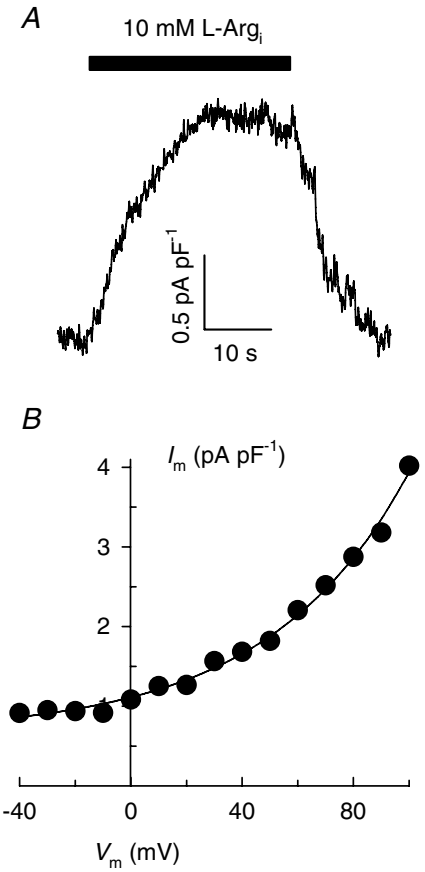

Figure 3. Intracellular L-Arg-activated currents in inside-out membrane patches excised from cardiac myocytes
A, outward current recorded at +40 mV by superfusing the patch intracellular side with 10 mM L-Arg. *B*, V_m dependence of current. Equation (1) (with a positive sign within the exponent) was fitted to the data. Currents follow the whole-cell convention, i.e. positive charges moving from the intracellular to the extracellular side of the patch are shown as a positive shift in current. Patch electrode tip diameter: 7.5 μm. Membrane capacitance: 11.6 pF.

To further characterize the molecular mechanism behind L-Arg import, currents generated by superfusing cardiac myocytes with L-lysine (L-Lys$_o$), L-ornithine (L-Orn$_o$), and D-arginine (D-Arg$_o$) were compared to those elicited with L-Arg$_o$. Figure 4 summarizes the V_m dependence of currents activated by extracellular application of these four amino acids at a concentration of 10 mM. L-Lys$_o$-, L-Orn$_o$- and L-Arg$_o$-sensitive currents displayed comparable current density levels and V_m dependence. Thus, these three L-amino acids appear to share the same mechanism to enter cardiac muscle cells. On the other hand, 10 mM D-Arg$_o$ produced small current levels, so that this amino acid was poorly (if at all) transported. In conclusion, cationic amino acids enter cardiac myocytes through a mechanism that shows stereospecificity for their L-isomers.

Voltage and L-Arg$_o$-concentration dependence of steady-state Arg import

To determine the apparent affinity with which L-Arg activates its flux across the cell plasma membrane, currents were measured in whole-cell voltage-clamped cardiac myocytes superfused with solutions containing L-Arg in the range of concentrations 1–50 mM. Figure 5*A* shows inward currents recorded from three different cells held at −40 mV and exposed to 1, 10 or 20 mM L-Arg$_o$. Comparison of the respective current levels indicates that 10 mM L-Arg$_o$-activated currents are far from saturation. The V_m dependence of current was determined at each L-Arg$_o$ concentration by applying the voltage-jump protocol (as described in Fig. 1) to generate I_m–V_m curves such those shown in Fig. 5*B*. Fitting eqn (1) to these I_m–V_m curves yielded best-fit values for parameter λ of 0.58 ± 0.06, 0.56 ± 0.02 and 0.48 ± 0.04, with 1, 10 and 20 mM L-Arg$_o$, respectively. Thus, changes in L-Arg$_o$ concentration as large as twentyfold did not significantly change the V_m dependence of current. Notice that all

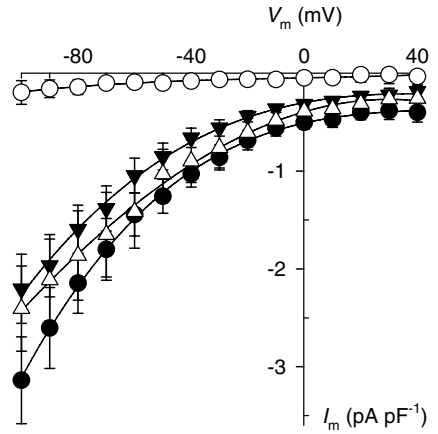

Figure 4. Selectivity of inward currents for cationic L-amino acids
I_m–V_m relationships were generated by application of the V_m-jump protocol to whole-cell voltage-clamped cardiac myocytes superfused with 10 mM L-Arg (●), L-Lys (△), L-Orn (▼), or D-Arg (○). Symbols represent the mean ± S.E.M. of 3 experiments for each condition.

I_m–V_m curves in Fig. 5*B* become almost parallel to the V_m axis at positive potentials.

Current levels for the entire range of L-Arg_o concentrations tested were fitted with Hill functions at each given V_m to obtain the L-Arg concentration for half-maximal activation of current ($K_{0.5}$), maximal current levels (I_{max}), and the Hill coefficient (n_H). The L-Arg_o concentration dependence of current is shown in

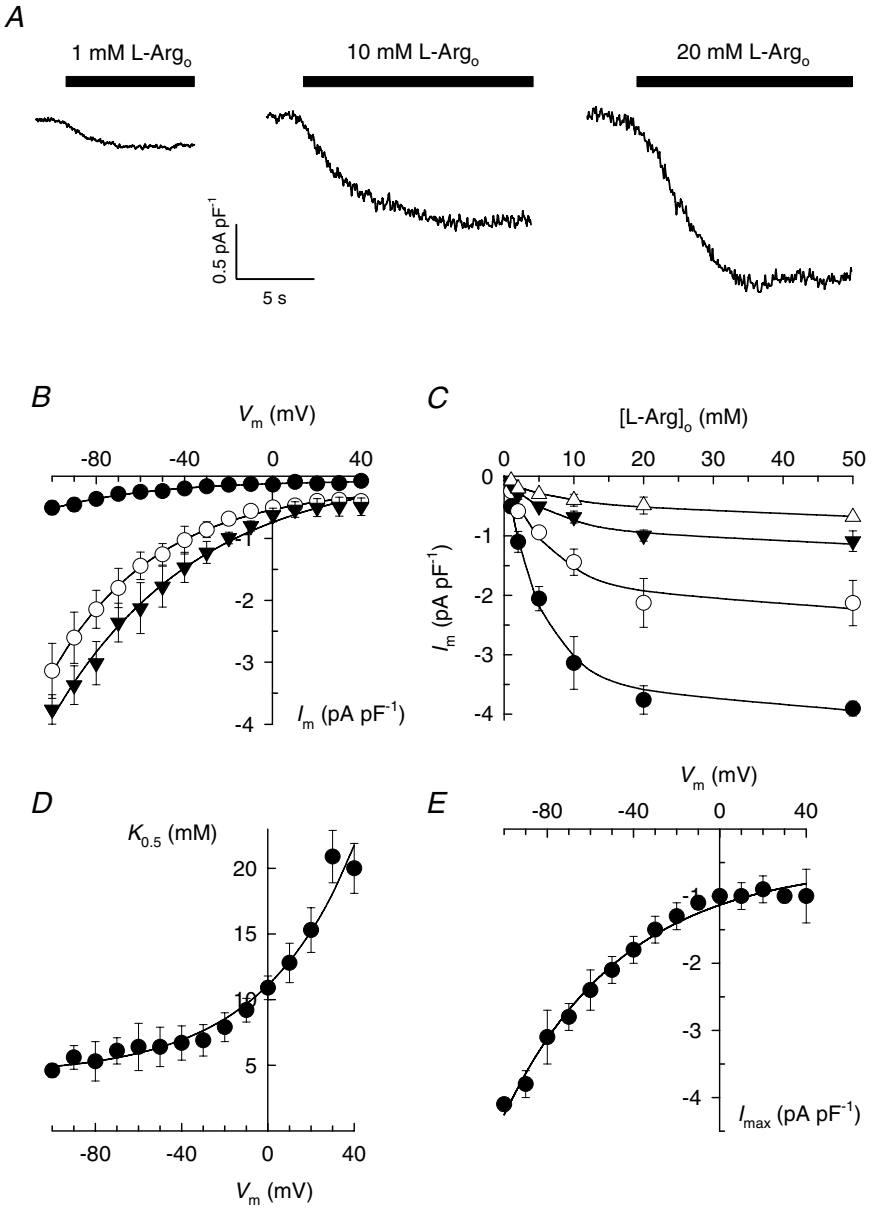

Figure 5. Membrane potential and L-Arg_o concentration dependence of current
A, extracellular L-Arg-activated currents in cardiac myocytes. Inward currents were elicited by superfusing the cells with increasing concentrations of L-Arg at −40 mV. *B*, summary I_m–V_m relationships for cells exposed to 1 (●; $n = 3$), 10 (○; $n = 5$), and 20 mM L-Arg (▼; $n = 4$). Curves represent fitting of eqn (1) to the data. *C*, L-Arg_o concentration dependence of current at −100 (●), −60 (○), −20 (▼) and +40 mV (△). Curves represent fitting of Hill equations with the following best-fit parameters: I_{max} (pA pF^{-1}): -4.1 ± 0.1, -2.4 ± 0.3, -1.3 ± 0.2 and -1.0 ± 0.4; $K_{0.5}$ (mM): 4.6 ± 0.5, 6.4 ± 1.8, 7.9 ± 1.1, and 20.0 ± 1.9; n_H: 1.30 ± 0.21, 1.19 ± 0.29, 1.02 ± 0.11, and 0.76 ± 0.19, for −100, −60, −20 and +40 mV, respectively. *D*, $K_{0.5}$–V_m relationship. $K_{0.5}$-values obtained as described in *C* were plotted *versus* cell membrane potential. The curve through the data points represents fitting of eqn (2). Assuming $z = 1$, best-fit parameters were found to be $A = 6.85 \pm 1.12$ mM, $\lambda = 0.60 \pm 0.10$, and $B = 4.25 \pm 0.81$ mM. Note that parameter *B* represents the value of $K_{0.5}$ as V_m approaches $-\infty$. *E*, I_{max}–V_m relationship. I_{max} values from the Hill analysis were plotted against V_m. Fitting eqn (1) to these data yielded a steepness factor $\lambda = 0.46 \pm 0.05$.

Fig. 5*C* for selected potentials along with best-fit curves (parameters are listed in the figure legend). It must be pointed out that n_H values showed no statistically significant deviation from 1.0. In fact, the average value for the entire range of V_m tested was found to be 1.01 ± 0.26 (S.D., $n = 15$).

Best-fit values of $K_{0.5}$ were plotted against the cell membrane potential as shown in Fig. 5*D*. Results show a V_m-dependent $K_{0.5}$ for L-Arg$_o$ activation of inward current. Apparent affinities decreased with depolarization, consistent with a positive cell interior antagonizing the inward movement of positive charges. The V_m dependence of $K_{0.5}$ was best described by the following empirical equation:

$$K_{0.5} = A \exp(\lambda z F V_m / RT) + B \quad (2)$$

The fraction of the membrane electric field dissipated during L-Arg$_o$-dependent reaction steps (λ) and the value of $K_{0.5}$ at zero V_m ($K^0{}_{0.5} = A + B$) were found to be 0.60 ± 0.10 and 11.1 ± 1.4 mM, respectively. The value of λ, which is comparable to the steepness of the I_m–V_m relationships (see above), indicates that charge-moving steps during Arg import dissipate approximately half of the electrical gradient across the cell membrane, a result consistent with binding of L-Arg$_o$ to sites in the protein located within the membrane dielectric.

The finding that a twentyfold change in L-Arg$_o$ concentration did not significantly modify the V_m dependence of current (Fig. 5*B*) suggests that steps other than Arg$_o$ binding/release must also contribute to the V_m dependence of Arg import. In line with this, I_{max} was found to be V_m dependent for the range of voltages tested (Fig. 5*E*). Notice that I_{max} increased (in absolute value) with hyperpolarization, consistent with a negative cell interior promoting the inward movement of positive charges.

Altogether, these results show that L-Arg$_o$, acting with low apparent affinity, activates inward currents in cardiac ventricular myocytes through a saturable, V_m-dependent process. A Hill coefficient value not significantly different from one suggests the presence of either just one L-Arg binding site or several identical, non-interacting sites for this amino acid.

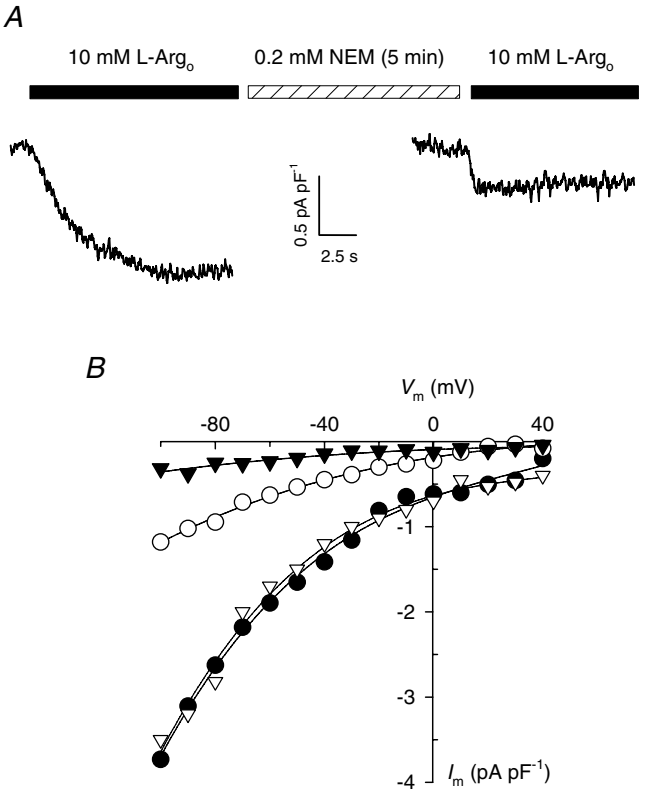

Figure 6. Effect of NEM on L-Arg$_o$-activated currents
A, 10 mM L-Arg$_o$-activated current in a whole-cell voltage-clamped cardiac myocyte held at −40 mV before and after application of 200 μM NEM for 5 min at 35°C. *B*, I_m–V_m relationships for currents measured before (●) and after 5 min (○) of NEM treatment for the cell in *A*. Also shown are I_m–V_m curves obtained from a different cell before (▽) and after a 7.5 min-long NEM treatment (▼).

Effect of *N*-ethylmaleimide (NEM) on L-Arg$_o$-activated currents

NEM was used as a general pharmacological tool to study the sensitivity of L-Arg currents to sulfhydryl reagents. Currents were activated with 10 mM L-Arg$_o$ in whole-cell voltage-clamped cardiac myocytes before exposure to and after removal of 0.2 mM NEM. As shown in Fig. 6*A* for a typical experiment, a 5 min-long NEM treatment produced a significant inhibition of L-Arg$_o$-induced current at the holding potential of −40 mV. I_m–V_m curves generated by applying the voltage-jump protocol before and after NEM treatment show that this inhibitor blocked current at all V_m tested (Fig. 6*B*, filled *versus* open circles). Since NEM binds irreversibly to sulfhydryl groups, only one incubation time with this reagent could be tested per cell. In addition, voltage-clamped myocytes did not survive a 10 min-long NEM incubation. Nonetheless, we found in three experiments that a 7.5 min-long exposure to 0.2 mM NEM was enough to inhibit 92 ± 5% of current at negative V_m. I_m–V_m curves from one of these experiments are also shown in Fig. 6*B* (open *versus* filled triangles).

Therefore, the totality of current measured upon perfusion of cardiac myocytes with L-Arg appears to be sensitive to brief incubations with 0.2 mM NEM, a concentration five- to tenfold lower than those needed to inhibit many transporters (see Discussion). This behaviour suggests the presence of readily accessible -SH groups that are important for L-Arg transport in the protein responsible for this process.

Discussion

This study reports novel L-Arg currents in whole-cell voltage-clamped cardiac ventricular myocytes. The magnitude of these currents encouraged biochemical and biophysical characterization of cardiac L-Arg transport in its native environment. The importance of studying L-Arg import is emphasized by the fact that cardiac myocytes are among the many cell types that do not have the biochemical machinery required for the *de novo* synthesis of arginine or to significantly recycle this amino acid from the co-product of NOS activity, citrulline (Hattori *et al.* 1995; Nagasaki *et al.* 1996).

Monovalent and divalent ion substitution experiments demonstrated that L-Arg is indeed the charge-carrying species that mediates these inward currents. This conclusion was independently supported by measurements of nitric oxide production in cells loaded with the fluorescent dye DAF-FM. We observed an increase in NO synthesis upon addition of L-Arg that was not paralleled by D-Arg or after incubation with a NOS inhibitor, a result that indicates L-Arg was transported into cardiac myocytes and converted by NOS into NO and citrulline.

Ion substitution experiments also showed that L-Arg import does not require Na^+, ionic gradients or ATP. Together with the finding that applying intracellular L-Arg elicited outward currents in giant patches excised from cardiac myocytes, these results strongly suggest that the movement of Arg molecules across the myocyte plasma membrane is passive, i.e. is driven by dissipation of the L-Arg electrochemical potential gradient.

Other amino acids, such as L-Lys and L-Orn, also produced inward currents of comparable magnitude and with similar V_m dependence to that displayed by L-Arg. On the other hand, D-Arg failed to produce any significant current, demonstrating the stereospecificity of the process for L-isomers of cationic amino acids. This ability to distinguish between enantiomers, a common feature of carriers, appears to be missing in channel proteins (Stein, 1990).

The study of the extracellular L-Arg concentration dependence of steady-state arginine import revealed a high-capacity, saturable process with a $K_{0.5}$ of 11 mM at zero V_m. The value of $K_{0.5}$ was found to be a function of V_m, decreasing to approximately 5 mM at hyperpolarizing voltages in the neighbourhood of the cardiac myocyte resting membrane potential. The V_m dependence of $K_{0.5}$ indicated that charge-moving steps during Arg transport dissipate approximately 50% of the electrical gradient across the cell membrane, a finding that may be explained by binding and unbinding of L-Arg_o to sites in the protein located within the membrane dielectric. Alternatively, a reaction step that rate-limits L-Arg binding may be V_m dependent. In this regard, since I_{max} also shows V_m dependence (with no signs of saturation at applied voltages up to −100 mV), a slow, V_m-dependent translocation step following L-Arg binding could be rate-limiting the transport of this amino acid. This view receives additional support from the experimental observation that a twentyfold change in L-Arg_o concentration did not significantly alter the V_m dependence of current (Fig. 5*B*). Finally, all steps involved in L-Arg transport, i.e. binding, translocation and release at the opposite side might move charge within the membrane electric field.

In terms of the protein responsible for L-Arg import, in the context of the known systems for cationic amino acid transport (see Introduction), system $B^{0,+}$ can be ruled out on the basis of the Na^+ independence of current, and systems b^+, $b^{0,+}$ and y^+L because of their high affinity for basic L-amino acids. The V_m dependence of I_m, $K_{0.5}$ and I_{max} resembles that of the CAT-1 member of the system y^+ family of cationic amino acid transporters, heterologously expressed in *Xenopus* oocytes (Kavanaugh, 1993). However, even though the high-affinity CAT-1 has been reported to be constitutively expressed in rat cardiac myocytes (Simmons *et al.* 1996), the L-Arg concentration dependence of current is consistent with the low-affinity, high-capacity CAT-2A described in mouse (Closs *et al.* 1993) and human (Closs *et al.* 1997) livers.

At this time, there are neither specific blockers for members of system y^+ nor commercially available antibodies for CAT-2A. Despite this, L-Arg currents were irreversibly inhibited by briefly exposing myocytes to submillimolar concentrations of NEM (Fig. 6). This sulfhydryl reagent, although non-specific, has been reported to rapidly and irreversibly inhibit cationic amino acid transport mediated by members of system y^+ at concentrations five- to tenfold lower than those required to block other carriers, exchangers, and pumps (Table 1). Moreover, ion channels do not usually show complete inhibition by NEM (Song *et al.* 2000; Papassotiriou *et al.* 2001) and, in fact, many show increased channel opening in the presence of this sulfhydryl reagent (Ahern *et al.* 1999; Yamaoka *et al.* 2000; Li *et al.* 2004). Thus, L-Arg_o-activated currents reported here might be entirely generated by L-Arg transport through a member of system y^+. Interestingly, neonatal rat cardiac myocytes show an increase in L-Arg uptake compatible with expression of the low-affinity transporter CAT-2A after a 24-h exposure to IL-1β and IFNγ (Simmons *et al.* 1996). However, the apparent affinity for L-Arg uptake reported by these authors is still tenfold higher than the value of $K^0_{0.5}$ for L-Arg activation of current determined with our freshly isolated and otherwise untreated adult rat cardiac myocytes. It must be pointed out that our experiments were not designed to detect a high-affinity current component. Assuming the simultaneous presence of CAT-1, its low capacity would probably produce small L-Arg-activated currents, hard to distinguish from background noise in our

Table 1. Inhibitory effect of NEM on selected transporters

Protein	[NEM] (mM)	Incubation time (min)	Temperature (°C)	Inhibition (%)
System y^+ [a]	0.2	6–10	25	~100
This study	**0.2**	**~8**	**35**	**>90**
System y^+L [a]	0.2	≥15	25	~0
Na^+,K^+-ATPase [b]	1	30	25	75–80
Choline carrier [c]	1	25	37	~100
ASC amino acid transporter [d]	1	60	37	50
Na^+–Ca^{2+} exchanger [e]	1.6	30	25	50

[a]Devés *et al.* (1993); [b]Fahn *et al.* (1966); [c]Devés & Krupka (1981); [d]Al-Saleh & Wheeler (1982); [e]Ren *et al.* 2001.

electrophysiological measurements. Final identification of the protein(s) as well as further characterization of this L-Arg transport process are underway.

Myocyte membrane depolarization due to cationic amino acid import is unlikely to have an effect *per se* on heart electrophysiology. Although currents in this work were mostly measured with 10 mM L-Arg_o to optimize signal-to-noise conditions, a total cationic amino acid concentration of 1 mM would be a more realistic approximation to physiological levels (see below). Resting adult rat ventricular cardiomyocytes have a V_m of −80 mV and an input resistance of ~40 MΩ in a Ca^{2+}-containing Krebs–Ringer buffer (Powell *et al.* 1980). From the I_m–V_m curve with 1 mM L-Arg_o in Fig. 5*B*, an inward current of 44 pA can be calculated at −80 mV, considering an average cell capacitance of 120 pF. This current would produce a cell membrane depolarization of only 1.8 mV. Even if a larger input resistance of 330 MΩ (Powell *et al.* 1980) is considered, the inward current above will depolarize the myocyte plasma membrane to −65 mV. Depolarization-activated, transient outward K^+ currents that influence cardiac action potentials are triggered by a much larger depolarization (Apkon & Nerbonne, 1991). Furthermore, L-Arg currents reported in the present study are upper-end estimates obtained under large electrochemical potential gradients (i.e. 'zero-*trans*' conditions). Thus, the depolarizing effect of Arg import may be even smaller in a cell containing a finite subsarcolemmal concentration of this amino acid.

With respect to the physiological relevance of a low-affinity Arg transport process in heart, the concentration of this amino acid in the plasma of healthy humans and rats ranges from 0.1 to 0.25 mM (van Haeften & Konings, 1989; Noeh *et al.* 1996). However, L-Lys and L-Orn, also present in the plasma, are transported with capacities and apparent affinities comparable to that of L-Arg (Kavanaugh, 1993; Devés & Boyd, 1998) and effectively compete with this amino acid for the carrier molecules. Thus, rat cardiac myocytes are probably sensing an 'effective' plasma cationic amino acid concentration of approximately 0.6 mM (Toback *et al.* 1973). A CAT-1-like transporter with a K_m of 0.1 mM would be turning over at 86% of V_{max} under these conditions. In addition, plasma levels of Arg and other amino acids can increase more than fivefold during catabolic states such as sepsis, trauma, severe burns, cancer and starvation (Harrison, 1991). Calculations based on two transporters acting in parallel, one with high affinity and low capacity, the other with low affinity and high capacity, show that at least half of the total transport activity proceeds through the low-affinity component when the concentration of

Table 2. Analysis of two hyperbolic current components acting in parallel

[L-CA] (mM)	I_{total} (pA pF^{-1})	I_{low} (%)
0.2	0.41	34
0.6	0.73	53
1.0	0.96	62
3.0	1.74	78
∞	4.00	90

The following sum of two Michaelis-Menten equations was used for these calculations:

$$I_{total} = I_{high} + I_{low} = \frac{I_{max,h}}{1+K_{m,h}/[L\text{-}CA]} + \frac{I_{max,l}}{1+K_{m,l}/[L\text{-}CA]}$$

where I_{total} is total current density; I_{high} and I_{low} are high-affinity, low-capacity, and low-affinity, high-capacity current components, respectively; $I_{max,h}$ and $I_{max,l}$ are the absolute values of maximal current densities, and $K_{m,h}$ and $K_{m,l}$ are the apparent affinities for the high- and low-affinity components, respectively; [L-CA] represents the extracellular concentration of cationic L-amino acids. Parameter values used in these calculations are as follows: $K_{m,h}$ = 0.1 mM (from Kavanaugh, 1993; at hyperpolarizing V_m); $I_{max,h}$ = 0.4 pA pF^{-1} (since at [L-CA] = 1 mM the high-affinity component should be saturated, the average current density obtained with 1 mM L-Arg at −80 mV in our experiments was used as an (over)estimate); $K_{m,l}$ = 5 mM (see Fig. 5*D* at −80 mV); $I_{max,l}$ = 3.6 pA pF^{-1} (Fig. 5*E* shows I_{max} values of ~4 pA pF^{-1} at large hyperpolarizing V_m; assuming this number represents the total contribution of both components, we subtracted 0.4 pA pF^{-1}). Note that lower values of $I_{max,h}$ will result in higher I_{low} percentages. No L-CA subsarcolemmal accumulation was considered for this analysis.

cationic amino acids is 0.6 mM, and this figure increases to 78% for a concentration of 3 mM (Table 2). Thus, a cardiac low-affinity, high-capacity transporter might modulate intracellular levels of Arg both physiologically and during pathological states. Interestingly, mRNA transcripts for the low-affinity CAT-2A accumulate in skeletal muscle in response to surgical trauma and food deprivation, although neither of the high-affinity system-y^+ transporters, CAT-1 and CAT-2B, are altered (Kakuda *et al.* 1998).

Under limiting substrate conditions, NOS is capable of generating superoxide radicals and peroxynitrite, a major contributor to myocardial depression (Ferdinandy *et al.* 2000). A high-capacity Arg transporter would ensure adequate L-Arg supply thus directing NOS enzymatic activity towards NO production and preventing the generation of by-products described to be responsible for cell oxidative damage. Thus, we hypothesize that a low-affinity, high-capacity Arg transport system might play a cardio-protective role during catabolic states. An increase in membrane Arg transport activity has been described in vascular endothelium, liver and intestine of critically ill patients, a finding interpreted as reflecting an increased Arg requirement in critical illness (Pan *et al.* 2004). Interestingly, improvement of clinical symptoms of cardiovascular disease is observed, upon oral L-Arg supplementation, once plasma levels for this amino acid have reached concentrations of 3–6 mM (Böger & Bode-Böger, 2001). Likewise, high doses of intravenous or oral Arg improve the outcome of patients with congestive heart failure (Koifman *et al.* 1995; Rector *et al.* 1996). These therapeutic Arg effects are likely to involve a low-affinity cationic amino acid transport process in heart.

References

Ahern GP, Hsu SF & Jackson MB (1999). Direct actions of nitric oxide on rat neurohypophysial K^+ channels. *J Physiol* **520**, 165–176.

Aidley DJ & Stanfield PR (1996). *Ion Channels*. Cambridge University Press, Cambridge, UK.

Al-Saleh EA & Wheeler KP (1982). Transport of neutral amino acids by human erythrocytes. *Biochim Biophys Acta* **684**, 157–171.

Apkon M & Nerbonne JM (1991). Characterization of two distinct depolarization-activated K^+ currents in isolated adult rat ventricular myocytes. *J Gen Physiol* **97**, 973–1011.

Balligand JL, Kelly RA, Marsden PA, Smith TW & Michel T (1993). Control of cardiac muscle cell function by an endogenous nitric oxide signaling system. *Proc Natl Acad Sci U S A* **90**, 347–351.

Böger RH & Bode-Böger SM (2001). The clinical pharmacology of L-arginine. *Annu Rev Pharmacol Toxicol* **41**, 79–99.

Bredt DS & Snyder SH (1994). Nitric oxide: a physiologic messenger molecule. *Annu Rev Biochem* **63**, 175–195.

Christensen HN (1964). A transport system serving for mono- and diamino acids. *Proc Natl Acad Sci U S A* **51**, 337–344.

Closs EI, Albritton LM, Kim JW & Cunningham JM (1993). Identification of a low affinity, high capacity transporter of cationic amino acids in mouse liver. *J Biol Chem* **268**, 7538–7544.

Closs EI, Gräf P, Habermeier A, Cunningham JM & Förstermann U (1997). Human cationic amino acid transporters hCAT-1, hCAT-2A and hCAT-2B: three related carriers with distinct transport properties. *Biochemistry* **36**, 6462–6468.

Collins A, Somlyo A & Hilgemann DW (1992). The giant cardiac membrane patch method: stimulation of outward Na^+-Ca^{2+} exchange current by MgATP. *J Physiol* **454**, 27–57.

Devés R, Angelo S & Chávez P (1993). *N*-Ethylmaleimide discriminates between two lysine transport systems in human erythrocytes. *J Physiol* **468**, 753–766.

Devés R & Boyd CAR (1998). Transporters for cationic amino acids in animal cells: discovery, structure, and function. *Physiol Rev* **78**, 487–545.

Devés R & Krupka RM (1981). Evidence for a two-state mobile carrier mechanism in erythrocyte choline transport: effects of substrate analogs on inactivation of the carrier by *N*-ethylmaleimide. *J Membr Biol* **61**, 21–30.

Fahn S, Hurley MR, Koval GJ & Albers RW (1966). Sodium-potassium-activated adenosine triphosphatase of *Electrophorus* electric organ. *J Biol Chem* **241**, 1890–1895.

Ferdinandy P, Danial H, Ambrus I, Rothery RA & Schulz R (2000). Peroxynitrite is a major contributor to cytokine-induced myocardial contractile failure. *Circ Res* **87**, 241–247.

Grocott-Mason R, Anning P, Evans H, Lewis MJ & Shah AM (1994). Modulation of left ventricular relaxation in isolated ejecting heart by endogenous nitric oxide. *Am J Physiol Heart Circ Physiol* **267**, H1804–H1813.

Harrison TR (1991). *Principles of Internal Medicine*. McGraw-Hill, New York.

Hattori Y, Shimoda S-I & Gross SS (1995). Effect of lipopolysaccharide treatment *in vivo* on tissue expression of argininosuccinate synthetase and argininosuccinate lyase mRNAs: relationship to nitric oxide synthase. *Biochem Biophys Res Commun* **215**, 148–153.

Hecker M, Sessa WC, Harris HJ, Anggard EE & Vane JR (1990). The metabolism of L-arginine and its significance for the biosynthesis of endothelium-derived relaxing factor: cultured endothelial cells recycle L-citrulline to L-arginine. *Proc Natl Acad Sci U S A* **87**, 8612–8616.

Hilgemann DW (1989). Giant excised cardiac sarcolemmal membrane patches: sodium and sodium-calcium exchange currents. *Pflugers Arch* **415**, 247–249.

Hobbs AJ, Higgs A & Moncada S (1999). Inhibition of nitric oxide synthase as a potential therapeutic target. *Annu Rev Pharmacol Toxicol* **39**, 191–220.

Kakuda DK, Finley KD, Dionne VE & MacLeod CL (1993). Two distinct gene products mediate y^+ type cationic amino acid transport in *Xenopus* oocytes and show different tissue expression patterns. *Transgene* **1**, 91–101.

Kakuda DK, Finley KD, Maruyama M & MacLeod CL (1998). Stress differentially induces cationic amino acid transporter gene expression. *Biochim Biophys Acta* **1414**, 75–84.

Kavanaugh MP (1993). Voltage dependence of facilitated arginine flux mediated by the system y^+ basic amino acid transporter. *Biochemistry* **32**, 5781–5785.

Kim JW, Closs EI, Albritton LM & Cunningham JM (1991). Transport of cationic amino acids by the mouse ecotropic retrovirus receptor. *Nature* **352**, 725–728.

Koifman B, Wollman Y, Bogomolny N, Chernichowsky T, Finkelstein A, Peer G, Scherez J, Blum M, Laniado S, Iaina A & Keren G (1995). Improvement of cardiac performance by intravenous infusion of L-arginine in patients with moderate congestive heart failure. *J Am Coll Cardiol* **26**, 1251–1256.

Kojima H, Nakatsubo N, Kikuchi K, Kawahara S, Kirino Y, Nagoshi H, Hirata Y & Nagano T (1998*a*). Detection and imaging of nitric oxide with novel fluorescent indicators: diaminofluoresceins. *Anal Chem* **70**, 2446–2453.

Kojima H, Sakurai K, Kikuchi K, Kawahara S, Kirino Y, Nagoshi H, Hirata Y & Nagano T (1998*b*). Development of a fluorescent indicator for nitric oxide based on the fluorescein chromophore. *Chem Pharm Bull* **46**, 373–375.

Li Y, Gamper N & Shapiro MS (2004). Single-channel analysis of KCNQ K^+ channels reveals the mechanism of augmentation by a cysteine-modifying reagent. *J Neurosci* **24**, 5079–5090.

MacLeod CL & Kakuda DK (1996). Regulation of CAT: cationic amino acid transporter gene expression. *Amino Acids* **11**, 171–191.

Mendes Ribeiro AC, Brunini TMC, Ellory JC & Mann GE (2001). Abnormalities in L-arginine transport and nitric oxide biosynthesis in chronic renal and heart failure. *Cardiovasc Res* **49**, 697–712.

Mitra R & Morad M (1985). A uniform enzymatic method for dissociation of myocytes from hearts and stomachs of vertebrates. *Am J Physiol Heart Circ Physiol* **249**, H1056–H1060.

Nagasaki A, Gotoh T, Takeya M, Yu Y, Takiguchi M, Matsuzaki H, Takatsuki K & Mori M (1996). Coinduction of nitric oxide synthase, argininosuccinate synthetase, and argininosuccinate lyase in lipopolysaccharide-treated rats. *J Biol Chem* **271**, 2658–2662.

Nawrath H, Wegener JW, Rupp J, Habermeier A & Closs EI (2000). Voltage dependence of L-arginine transport by hCAT-2A and hCAT-2B expressed in oocytes from *Xenopus laevis*. *Am J Physiol Cell Physiol* **279**, C1336–C1344.

Nichols CG & Lederer WJ (1991). Adenosine triphosphate-sensitive potassium channels in the cardiovascular system. *Am J Physiol Heart Circ Physiol* **261**, H1675–H1686.

Noeh FM, Wenzel A, Harris N, Milakofsky L, Hofford JM, Pell S & Vogel WH (1996). The effects of arginine administration on the levels of arginine, other amino acids and related amino compounds in the plasma, heart, aorta, vena cava, bronchi and pancreas of the rat. *Life Sci* **58**, 131–138.

Pan M, Choudry HA, Epler MJ, Meng Q, Karinch A, Lin C & Souba W (2004). Arginine transport in catabolic disease states. *J Nutr* **134**, 2826S–2829S.

Papassotiriou J, Eggermont J, Droogmans G & Nilius B (2001). Ca^{2+}-activated Cl^- channels in Ehrlich ascites tumor cells are distinct from mCLCA1, 2 and 3. *Pflugers Arch* **442**, 273–279.

Peluffo RD (2004). Characterization of electrogenic arginine transport in rat cardiomyocytes. *Biophys J* **86**, 614a.

Peluffo RD (2005). L-arginine-activated currents in rat cardiomyocytes are consistent with cationic amino acid transport *via* CAT-2A. *Biophys J* **88**, 594a.

Powell T, Terrar DA & Twist VW (1980). Electrical properties of individual cells isolated from adult rat ventricular myocardium. *J Physiol* **302**, 131–153.

Rector TSP, Bank AJM, Mullen KAR, Tschumperlin LKR, Sih RM, Pillai KM & Kubo SHM (1996). Randomized, double-blind, placebo-controlled study of supplemental oral L-arginine in patients with heart failure. *Circulation* **93**, 2135–2141.

Ren X, Kasir J & Rahamimoff H (2001). The transport activity of the Na^+–Ca^{2+} exchanger NCX1 expressed in HEK 293 cells is sensitive to covalent modification of intracellular cysteine residues by sulfhydryl reagents. *J Biol Chem* **276**, 9572–9579.

Simmons WW, Closs EI, Cunningham JM, Smith TW & Kelly RA (1996). Cytokines and insulin induce cationic amino acid transporter (CAT) expression in cardiac myocytes. *J Biol Chem* **271**, 11694–11702.

Smith PA, Sakura H, Coles B, Gummerson N, Prok S & Ashcroft FM (1997). Electrogenic arginine transport mediates stimulus-secretion coupling in mouse pancreatic β-cells. *J Physiol* **499**, 625–635.

Song J, Jang YY, Shin YK, Lee C & Chung S (2000). N-Ethylmaleimide modulation of tetrodotoxin-sensitive and tetrodotoxin-resistant sodium channels in rat dorsal root ganglion neurons. *Brain Res* **855**, 267–273.

Sperandeo MP, Borsani G, Incerti B, Zollo M, Rossi E, Zuffardi O, Castaldo P, Taglialatela M, Andria G & Sebastio G (1998). The gene encoding a cationic amino acid transporter (SLC7A4) maps to the region deleted in the velocardiofacial syndrome. *Genomics* **49**, 230–236.

Stein WD (1990). *Channels, Carriers, and Pumps: an Introduction to Membrane Transport*. Academic Press, San Diego.

Toback FG, Mayers AM & Lowenstein LM (1973). Alterations in renal and plasma amino acid concentrations during renal compensatory growth. *Am J Physiol* **225**, 1247–1251.

van Haeften TW & Konings CH (1989). Arginine pharmacokinetics in humans assessed with an enzymatic assay adapted to a centrifugal analyzer. *Clin Chem* **35**, 1024–1026.

Van Winkle LJ & Campione AL (1990). Functional changes in cation-preferring amino acid transport during development of pre-implantation mouse conceptuses. *Biochim Biophys Acta* **1028**, 165–173.

Wu GY & Brosnan JT (1992). Macrophages can convert citrulline into arginine. *Biochem J* **281**, 45–48.

Yamaoka K, Yakehiro M, Yuki T, Fujii H & Seyama I (2000). Effect of sulfhydryl reagents on the regulatory system of the L-type Ca channel in frog ventricular myocytes. *Pflugers Arch* **440**, 207–215.

Acknowledgements

This work was supported by National Institutes of Health Grant HL076392 and by a Scientist Development Grant from the American Heart Association, National branch. The author wishes to thank the technical assistance of Ms Renee Green, and Drs John Reeves, Andrew Harris, and Joshua Berlin for carefully reading earlier versions of the manuscript and providing useful comments and suggestions. Dr Berlin's help with the confocal microscopy studies on DAF-FM loaded myocytes is also acknowledged.